



SCHOOL of
GRADUATE STUDIES
EAST TENNESSEE STATE UNIVERSITY

East Tennessee State University
Digital Commons @ East
Tennessee State University

Electronic Theses and Dissertations

Student Works

12-2009

Determination of the Activation Parameters of Reaction Between $[\text{Fe}(\text{CN}_6)]^{-4}$ and $\text{K}[\text{Co}(\text{HEDTA})\text{NO}_2]$.

Sammy Eni Eni

East Tennessee State University

Follow this and additional works at: <https://dc.etsu.edu/etd>

 Part of the [Organic Chemistry Commons](#)

Recommended Citation

Eni Eni, Sammy, "Determination of the Activation Parameters of Reaction Between $[\text{Fe}(\text{CN}_6)]^{-4}$ and $\text{K}[\text{Co}(\text{HEDTA})\text{NO}_2]$." (2009). *Electronic Theses and Dissertations*. Paper 1798. <https://dc.etsu.edu/etd/1798>

This Thesis - Open Access is brought to you for free and open access by the Student Works at Digital Commons @ East Tennessee State University. It has been accepted for inclusion in Electronic Theses and Dissertations by an authorized administrator of Digital Commons @ East Tennessee State University. For more information, please contact digilib@etsu.edu.

The Determination of the Activation Parameters of Reaction Between $[\text{Fe}(\text{CN})_6]^{-4}$ and
 $\text{K}[\text{Co}(\text{HEDTA})\text{NO}_2]$

A thesis
presented to
the faculty of the Department of Chemistry
East Tennessee State University
in Partial Fulfillment
of the requirements for the degree
Master of Science in Chemistry

by
Sammy Eni Eni
December 2009

Dr. Jeffrey Wardeska, Chair

Dr. Ningfeng Zhao

Dr. Yu-Lin Jiang

Keywords: Activation parameters, $[\text{Fe}(\text{CN})_6]^{-4}$, $\text{K}[\text{Co}(\text{HEDTA})\text{NO}_2]$.

ABSTRACT

Determination of the Activation Parameters of Reaction Between $[\text{Fe}(\text{CN})_6]^{-4}$ and $\text{K}[\text{Co}(\text{HEDTA})\text{NO}_2]$

by

Sammy Eni Eni

The kinetics of the oxidation of $[\text{Fe}(\text{CN})_6]^{-4}$ by $\text{K}[\text{Co}(\text{HEDTA})\text{NO}_2]$ was studied in order to get the mechanism and the activation parameters of the reaction. Using a freshly-made Na_3PO_4 solution as the reaction medium with a pH of 6.00 the ionic strength was maintained at 0.10 M and the buffer molarity was 0.001 M.

The rate constant (k_{obs}) of the reaction between $[\text{Fe}(\text{CN})_6]^{-4}$ and $\text{K}[\text{Co}(\text{HEDTA})\text{NO}_2]$ was determined at temperatures of 25.0⁰C, 27.5⁰C, 30.0⁰C, 35.0⁰, and 40.0⁰C. We explored this reaction by monitoring the evolution of ferricyanide, $[\text{Fe}(\text{CN})_6]^{-3}$, spectroscopically for which $\epsilon_{420} = 1023 \text{ cm}^{-1} \text{ M}^{-1}$ by recording the absorbance as a function of time at 420 nm wavelength. The data were plotted and results analyzed to give activation parameters, energy of activation (E_a), entropy of activation (ΔS^\ddagger), and enthalpy of activation (ΔH^\ddagger) for the two reacting complexes under the specified reaction conditions. Based on previous results, an outer-sphere electron-transfer pathway and a first order rate of reaction for each of the reacting species¹ have been proposed.

ACKNOWLEDGEMENTS

Thanking God for strength and guidance throughout my life. The support and encouragements from my family especially my uncle Mr. Oscar Obase Ndoh, my parents Mr. Eni Eni Patrick, and Mrs. Eni Helen Ndoh has been second to none. My special gratitude to Dr. Jeffrey Wardeska for initiating, directing this project, and for fatherly guidance throughout my study. The author also likes to thank Mrs. Susan Campbell, Mrs. Barbara Rasnick, and other staff and faculty of the chemistry department at East Tennessee State University for help at all levels.

CONTENTS

	Page
ABSTRACT.....	2
LIST OF TABLES.....	6
LIST OF FIGURES.....	7
Chapter	
1. INTRODUCTION.....	8
2. EXPERIMENTAL METHODS.....	14
Instrument, Glassware, and Miscellaneous Materials.....	14
Reagent Grade Stock Chemicals.....	14
Cleaning Solutions.....	14
Synthesis of $K[Co(HEDTA)NO_2]^-$	15
Characterization.....	16
Kinetics.....	17
3. RESULTS.....	21
4. DISCUSSION.....	32
BIBLIOGRAPHY.....	39
APPENDICES.....	40
Appendix A: The Data for Absorbance vs Temperatures for 1:1 Molar Ratio.....	40
Appendix B: The Data for Absorbance vs Temperatures for 1:10 Molar Ratio.....	41
VITA.....	42

LIST OF TABLES

Table	Page
1. Percent of Reaction Completion Between Ferrocyanide and Co Complex.....	24
2. The Observed Rate Constants at Different Temperatures for 1:1 Ratio.....	27
3. The Observed Rate Constants at Different Temperatures for 1:10 Ratio	31
4. Activation Parameters for 1:1 and 1:10 Molar Ratios.....	35

LIST OF FIGURES

Figure	Page
1. Schematic Representation of Reaction Between $\text{Fe}(\text{CN})_6^{4-}$ and $[\text{Co}(\text{HEDTA})\text{NO}_2]^-$..	13
2. The plot of the Percent Transmittance vs wave numbers of $\text{K}[\text{Co}(\text{HEDTA})\text{NO}_2]$	22
3. The UV Spectrum of $[\text{Co}(\text{HEDTA})\text{NO}_2]^-$ at Wavelength 400-600nm at pH 6.00.....	25
4. Plot of Absorbance vs Time of Reaction Between $\text{Fe}(\text{CN})_6^{4-}$ and $[\text{Co}(\text{HEDTA})\text{NO}_2]^-$..	26
5. Plot of $\ln(\text{A}_{\text{max}}-\text{A})$ vs Temperatures for a 1:1 Molar Ratio.....	27
6. Plot of $\ln(\text{K})$ vs $1/\text{T}$ for 1:1 Molar Ratio.....	28
7. Plot of $\ln(\text{K}/\text{T})$ vs $1/\text{T}$ for 1:1 Molar Ratio.....	29
8. Plot of $\ln(\text{A}_{\text{max}}-\text{A})$ vs Temperature In a 1:10 Molar Ratio.....	30
9. Plot of $\ln(\text{K})$ vs $1/\text{T}$ for 1:10 Molar Ratio.....	31
10. Plot of $\ln(\text{K}/\text{T})$ vs $1/\text{T}$ for 1:10 Molar Ratio.....	32

CHAPTER 1

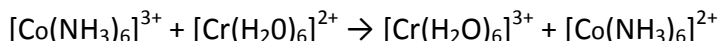
INTRODUCTION

Modern day chemistry has seen tremendous improvements both in novelties and already existing reactions, particularly with the understanding of their underlying mechanisms. Mechanisms are simply pathways that reactants undergo in order to get to their products.

Reactions are widely classified into groups based on various common intrinsic properties. Addition, substitution, acid-base, and oxidation-reduction (redox) reactions are just a few common chemical reactions. Our area of interest is redox reactions that involve the loss and gain of electrons from species. The species that gains electrons is the oxidizing agent while the other that loses the electron is the reducing agent. The two species involved in the reaction have to be in close proximity and the electrons are then transferred either through a ligand or the metal center based on the plausible mechanism. Details of the mechanism can be acquired by exploring parameters like the rate of electron transfer, the equilibrium constant between the species and the order of the reaction.

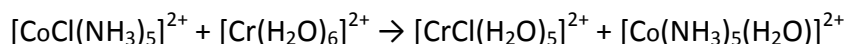
Two basic mechanisms of redox reactions exist; inner-sphere and outer-sphere. Outer-sphere mechanism also known as non-bonded electronic transfer. These refers to the transfer of electrons between chemical moieties that remain as separate chemical species before, during, and also after the transfer is completed. Inner-sphere mechanism, also known as self-exchange electronic transfer, occurs when two sites undergoing electronic transfer are connected through a chemical bridge through which the electronic exchange takes place.

An example for an outer-sphere mechanism is;



There is transfer of an electron from Cr to Co with no bridging between the complexes.

An example of an inner-sphere mechanism is;



Here the Cl forms a bridge between the two complexes which facilitates electron-transfer.

The mechanism of a reaction is the detailed manner in which the reaction proceeds with emphasis on the number and nature of the steps involved in the reaction. There are various means of elucidating the mechanism that include determining the rate law, the effect on the rate constant by varying the structure of reactants (linear free energy relations), and also parameters like temperature and pressure. Experiments and good chemical intuition also have a great role to play.

For a mechanism to be considered plausible, its individual steps have to add up to an overall balanced equation. The individual steps with their respective rate constants must all be balanced with respect to charges and atoms. The over-all reaction must produce a rate law that is identical to the experimental rate law. Other parameters and trends could also be taken into consideration in order to maximize the possibility of getting the right mechanism. This especially applies to the rate determining step for instance; any species that occurs in the reaction stoichiometry but not in the rate law must react in the step preceding the rate determining step.

The crystal field stabilization theory helps determine both the geometry of the complex and its stability that is acquired from the d-orbital electronic arrangement of metal. Crystal field stabilization energy is the energy gained by the complex due to the splitting of the d-orbital into t_{2g} and e_g sublevels. The energy difference between these two sublevels is dependent on various parameters including the ligand itself. If the ligand field strength is large, the electrons will pair up and fill the lower t_{2g} sublevel before getting into the e_g sublevel. This is the 'low-spin' case. In the 'high spin' case, the field strength is small and the electrons can partially fill both e_g and t_{2g} sublevels before pairing.

The Fe in ferrocyanide and Co in the HEDTA complex (HEDTA is 2-hydroxyethyl-ethylenediaminetriacetate) both have a low-spin $3d^6$ electronic configuration. The cobalt is in its +3 oxidation state while the Fe is in its +2 oxidation state. Their electrons occupy the low energy t_{2g} orbital because they are low-spin and all six electrons in the two species are paired.

There exist many techniques used to analyze the products from redox reactions. The UV/Visible electron absorption spectroscopy is mostly used due to its simplicity and overall accuracy. Species absorbs energy from a certain portion of the electro-magnetic spectrum based on their electronic configuration. By measuring the ratio of the amount of energy transmitted through the sample and a reference the absorbance of the species can be acquired. Using the Beer-Lambert law,

$A = c \epsilon l$, where ϵ is the Extinction coefficient and l is the cell path length. Absorbance (A) is proportional to the concentration of the sample. The rate of a reaction is the change

with time of the concentration of one of the reactants or one of the products of the reaction; that is,

Rate is $d[\text{reactants}]/dt$.

Suppose that the rate of a reaction depends only on the concentration of species A and B. The proportionality factor k , relating rate to the concentration of [A] and [B], the rate equation is

$$\text{Rate of reaction (V)} = k[A]^a[B]^b \text{ where } k \text{ is the specific rate constant.}$$

The values of a and b determine the order of the reaction. The overall order is the sum of a and b .

The rate of reaction is measured mostly by the initial-rate method where the initial concentrations of the species reacting are accurately known and used. The steady-state approach is also used especially in very complex systems. Many times a 'pseudo first order' is used in conducting kinetic experiments. Here one of the reactants is in a concentration at least 10 times in excess of the species of interest. The excess reactant is assumed to stay relatively unchanged in the course of the reaction. As the reaction proceeds, it either approaches equilibrium or continues until the limiting reagent is consumed. Other parameters like temperature or pressure could be used to change equilibrium position.

From previous research¹ on the mechanism of the reaction between ferrocyanide and $[\text{Co}(\text{HEDTA})\text{NO}_2]^-$, the observe rate constant, k_{obs} , the electronic transfer rate constant k_2 and the rate constant for the formation of the iron-pair, k_{os} , of the reaction of the species at a given temperature (25⁰ C) were all determined using the literature procedure. It was realized that the rate constants were not affected by pH and that each species exhibited a first order rate of

reaction. As a result of the analyses of the results and data, the outer-sphere mechanism was also proposed as the means of electron transfer.

In early 1974, the Kinetics of the reaction of $[\text{Co}(\text{HEDTA})]^{2-}$ with ferricyanide was studied² in which the equilibrium constant of the formation reaction and the rate constant of the dissociation reaction of the intermediate at an ionic strength of 0.66 M were explored in detail. In this research, it was concluded that the reaction between the species proceeded with two consecutive steps; the first step was the formation of a metastable binuclear intermediate through an inner-sphere mechanism, while the second step included the dissociation of the intermediate to produce ferrocyanide and the oxidized Co complex. This study led to many other studies of the reaction of ferricyanide with several cobalt aminopolycarboxylate complexes in order to ascertain how changes in the nature of aminopolycarboxylates influenced the features of their reactions².

Our research is aimed at exploring the reduction and oxidation between $[\text{Fe}(\text{CN})_6]^{-4}$ and $[\text{Co}(\text{HEDTA})\text{NO}_2]^-$ by determining the activation parameters of the reaction. These molecules contain transition metal ions with octahedral geometry and all have a low-spin 'd⁶' electron configuration. Looking closely, we realize that the two complexes are negatively charged and it is intriguing in that in spite of repelling each other (as we expect like charges to do) they transfer electrons between themselves!

With an already existing guideline for our synthesis of $\text{K}[\text{Co}(\text{HEDTA})\text{NO}_2]$, necessary modifications led to a higher yield and a purer product. Potassium ferrocyanide is a stock compound, the synthesized crystalline cobalt complex was verified through analytical methods

and comparing results with literature values proved rather satisfactory. Next we explored the reaction of our cobalt complex with ferrocyanide by monitoring the evolution of ferricyanide $[\text{Fe}(\text{CN})_6]^{-3}$ at 420 nm, with $\epsilon_{420} = 1023 \text{ dm}^3 \text{ mol}^{-1} \text{ cm}^{-1}$. We then carried out the reaction at temperatures of 25.0°C , 27.5°C , 30.0°C , 35.0°C , and 40.0°C . We were able to replicate each set of data, and by plotting we deduced the activation parameters for the reaction.

The overall reaction between the two species is represented in the Figure 1 below;

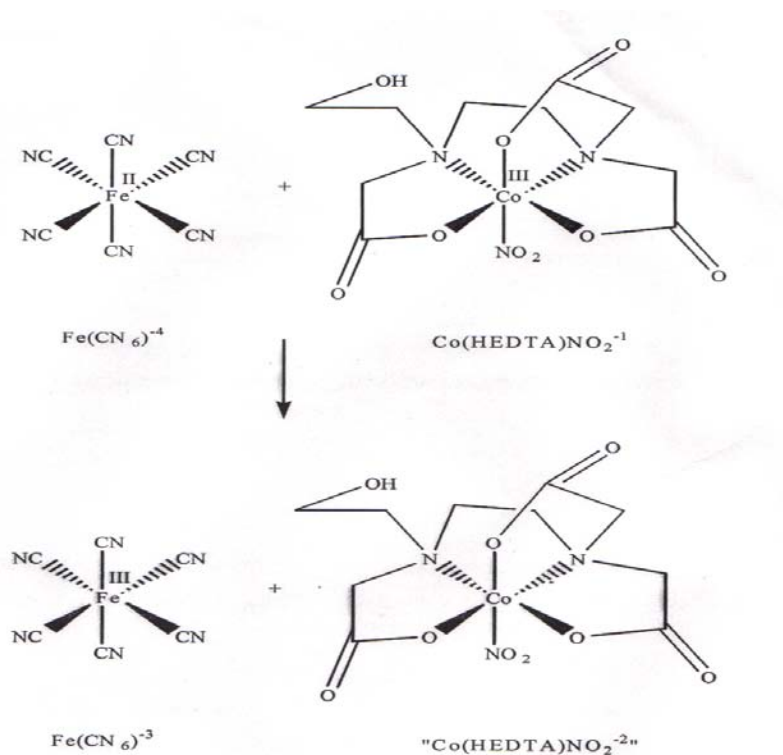


Figure 1. Schematic Representation of Reaction Between $\text{Fe}(\text{CN})_6^{4-}$ and $[\text{Co}(\text{HEDTA})\text{NO}_2]^{-1}$

CHAPTER 2

EXPERIMENTAL METHODS

Instruments, Glass-ware, and Miscellaneous Materials

The following instruments and glass-ware were used in the experiment: UV/Vis/IR spectrometer with a temperature bath, Fisher pH meter, Microsoft Excel, 500 μ L syringe , 10.0 ml volumetric flasks, 100 ml volumetric flask, 1.0 cm path length cuvettes, rubber septa, and 22 gauge syringe needles.

Reagent Grade Stock Chemicals

The reagent grade stock chemicals used included the following; cobalt chloride hexahydrate, $\text{CoCl}_2 \cdot 6\text{H}_2\text{O}$, (2-hydroxyethyl) - ethylene diaminetriacetic acid (HEDTA), and sodium nitrite NaNO_2 . We also used glacial acetic acid, potassium hexacyanoferrate(II), sodium nitrate (NaNO_3), sodium phosphate monobasic Na_2HPO_4 , Standard buffer solutions, dilute HCl, sodium hydroxide, isopropanol, and ethanol. All the chemicals used were ACS reagent grade chemicals and were used as obtained.

Cleaning Solutions

In order to prevent staining of the glassware with Prussian-blue complex, care must be taken while cleaning. A solution of NaOH and isopropanol was prepared.

De-ionized water was first used to remove excess ferrocyanide. Then a saturated solution of NaOH in isopropanol was used to wash the glassware. Distilled water was used to

rinse off the isopropanol, then the glassware was soaked in dilute HCl before finally rinsed with distilled water.

Synthesis of $K[Co(EDTA)NO_2]$

A 27.82 g of HEDTA was weighed and added to a solution of 12.03 g (0.33 moles) NaOH in a 250.0 mL beaker with 50.0 mL of deionized water. The solutions were mixed thoroughly which produced $3 Na^+HEDTA^{-3}$. This solution was then added to 24.00 g (0.1000 moles) of $CoCl_2 \cdot 6H_2O$ in a 500.0 mL beaker. Enough distilled water was added to ensure complete solution. $NaNO_2$, 15.00 g (0.2174 moles), was added drop-wise to the solution. The solution effervesces, and adding $NaNO_2$ quickly causes the solution to foam excessively. Glacial acetic acid (70.0 mL) was added and the solution mixed thoroughly.

Most of the liquid was slowly evaporated at room temperature. The liquid was decanted and the solid was washed with ice water. Repeated washing was required to remove impurities of Co^{+2} and nitrite ions because K^+ would be added in the next step. Excess Co^{+2} and nitrite in combination with K^+ , will precipitate as $K_3Co(NO_2)_6$. The solid was re-dissolved in distilled water at room temperature. Approximately 15.0 mL of water in excess was added to completely dissolve the solid. To this solution, 29.76 g (0.4000 moles) of KCl was added and mixed thoroughly. The precipitate was then re-crystallized at room temperature, the liquid was decanted, and the solid washed with cold distilled water. Repeated dissolving, re-crystallization, and washing were needed to achieve high purity. After the final re-crystallization, the product

was washed with 50/50 ethanol-water solution and dried under a vacuum at 70.0⁰ C. This gave a product yield of 89.9%.

The amount of H₂O in our product was determined by drying a 0.5073 g of our product in a 100.0⁰ C oven for 10 minutes. The solid was then cooled and weighed. The process was repeated until the mass was constant. The constant mass was 0.5035 g. This gave a percent weight loss (amount of water) of 0.749%. This meant that our product had very little amount of water and so it was dry enough for the reaction with ferrocyanide.

Characterization

The first characterization was done by measuring the electronic absorption spectrum of a 0.003676 M solution of K[Co(HEDTA)NO₂] that gave a maximum absorbance (A_{max}) of 0.847 at 495 nm. Using Beer's law, the molar extinction coefficient was calculated to 230.4 dm³mol⁻¹cm⁻¹ that was compared to the literature value of 232.00 dm³mol⁻¹cm⁻¹ indicating a purity of 99.3%, and this was an indication that Beer's Law was obeyed. This first characterization confirmed the product to be the K[Co(HEDTA)NO₂].

The second characterization was done with the Infrared (IR) spectrum to determine if the nitro group was present in our complex and also to determine if it existed as a nitro (NO₂) or as a nitrito (ONO). This was done by grinding 0.25 g of our complex with 1 g of KBr. The sample was crushed and ground to reduce particle size and also to produce a homogenous mixture. A small pellet of our crushed product was made by applying a pressure of 20,000 psi using the pellet press.

This pellet was inserted in the IR and showed a peak at 1334.15 cm^{-1} . This confirmed two things about the complex; first, it confirmed the presence of a nitro group in the complex and second, it confirmed the kind of bonding the nitro group had with the Co complex. If the NO_2 group present in the complex had a N bonded to the Co center, we have a nitro function, but if the Oxygen is bonded to the metal center, we have a nitrito (ONO) function. The spectrum is shown in Figure 2.

The second characterization confirmed the presence of the nitro group in our complex and also confirmed the type of bonding existing between the NO_2 and the Co center.

Kinetics

For our kinetic measurements to be meaningful, it was necessary to prepare a solution with constant molarity and ionic strength (μ) that was to be our reaction medium. The buffer was prepared by dissolving 0.8500 g (0.10 moles) of NaNO_3 and 0.142 g (0.01 moles) of Na_2HPO_4 in 85.0 mL of distilled water. This was titrated to a desired pH with dilute HCl. The buffer solution was transferred to a 100.0 mL volumetric flask and adjusted to the mark with distilled water. This gave a buffer solution with an ionic strength of 0.1 M, and a buffer molarity of 0.01 M and pH of 6.00. The buffer solution was used as the reaction medium.

Because ferrocyanide is oxidized by O_2 , the reaction was carried out without O_2 . A known weight of the dry complex was placed in a clean 10mL volumetric flask and sealed with a septum. A 22 gauge needle was then inserted in the top. A second needle attached to an argon supply at 1 atm was also inserted. Argon flushed the container for 2 minutes.

The argon supply was removed and a venting needle from the degassing apparatus was inserted. While keeping a positive pressure of approximately 2 atm, the apparatus was inverted so that the buffer solution flowed into the 10.0 mL volumetric flask. When the volumetric flask was filled to the mark, both needles were removed from reagent flask.

Ferrocyanide and the Co complex by themselves were measured for stability. Solutions with known concentrations of ferrocyanide were prepared as above at pH 6.00. The solutions were monitored over a period of 2 hours at 420.0 nm against a control buffer solution. A solution of $\text{K}[\text{Co}(\text{HEDTA})\text{NO}_2]^-$ was also prepared and a spectrum observed from 360.0 nm to 600.0 nm over a period of 2 hours to determine if the Co complex is stable.

The reaction between $[\text{Co}(\text{HEDTA})\text{NO}_2]^-$ and ferrocyanide was observed from the oxidation of ferricyanide by recording the absorbance at 420.0 nm as a function of time at various temperature. The $[\text{Co}(\text{HEDTA})\text{NO}_2]^-$ also absorbs energy in the region at 420.0 nm. Therefore the reference cell contained an equal concentration of the Co complex as the reaction cell. To determine if the reaction between the species went to completion, or reached equilibrium, the reaction was carried at different concentrations and the maximum absorbance was compared with literature values and the percent reaction completion was calculated.

First, the buffer was prepared and degassed by the procedure described earlier. A ferrocyanide solution was prepared by placing 1.0983 g (0.0026 moles) of $\text{K}_4[\text{Fe}(\text{CN})_6]$ in a 10.0 mL volumetric flask, (in constant temperature water bath). The flask was filled with the buffer solution as described earlier in the section above.

In a second 10.0 mL volumetric flask, 0.0041 g (9.660×10^{-6} moles) of $\text{K}[\text{Co}(\text{HEDTA})\text{NO}_2]$ was prepared in the same fashion. Adequate time was provided to allow the species to dissolve. Two quartz cuvettes were flushed with argon and sealed with a septum. The solution in the reference cuvette was made by using a 500 μL glass syringe to add 0.800 mL of the $[\text{Co}(\text{HEDTA})\text{NO}_2]^-$ solution. Then 0.500 mL of the buffer was added. The reaction cuvette was prepared by using a 500 μL glass syringe to inject 0.800 mL of $[\text{Co}(\text{HEDTA})\text{NO}_2]^-$. Using a separate syringe, 0.500 mL $[\text{Fe}(\text{CN})_6]^{-4}$ was injected. The cuvette was inverted twice to mix the reactants. Quickly, the cuvette was placed into the spectrometer and the scan was started. The reaction was studied at temperature of 25.0°C , following the increase in absorbance at 420 nm. After approximately 6 minutes, the absorbance began to level off. After several minutes, the absorbance was checked again. This process was repeated until the absorbance did not change. The final reading was taken as A_{max} . This experiment was repeated leaving the ferrocyanide concentration the same and decreasing the amount of $[\text{Co}(\text{HEDTA})\text{NO}_2]^-$. The ferrocyanide was 0.1M and remained constant. The $[\text{Co}(\text{HEDTA})\text{NO}_2]^-$ concentrations measured were 3.0×10^{-4} M, 4.5×10^{-4} M, 6.0×10^{-4} M and 2.0×10^{-3} M. An additional experiment was done in which 2.0×10^{-3} M $[\text{Co}(\text{HEDTA})\text{NO}_2]^-$ was reacted with 0.0090 M $[\text{Fe}(\text{CN})_6]^{-4}$.

The rate constants of the reaction at various temperatures were determined. Reagent solutions were prepared in the above-mentioned procedure. The $[\text{Fe}(\text{CN})_6]^{-6}$ solution contained 1.3728 g (0.00325 moles) $\text{K}_4[\text{Fe}(\text{CN})_6]$ in 10.0 mL of the buffer solution. The Co complex solution contained 0.0066g (1.55×10^{-5} moles) of $\text{K}[\text{Co}(\text{HEDTA})\text{NO}_2]$ in 10.0 mL of the buffer solution. In this set of kinetic experiments, the Co complex concentration remained at 6.00×10^{-4} M in the reagent cuvette while the reference cuvette had distilled water. This was accomplished by

injecting 0.500 mL of the Co complex solution using a 500 μ L glass syringe and 0.80mL of the buffer solution to a sealed and argon-flushed cuvette. These cuvettes were placed in the temperature bath for 10 minutes in order for both solutions to have the same temperature. The reaction cuvette contained 0.80 mL of the ferrocyanide solution and 0.50 mL of the $[\text{Co}(\text{HEDTA})\text{NO}_2]^-$ solution. These kinetic studies were performed at pH 6.00 and temperatures of 25.0⁰ C, 27.5⁰ C, 30.0⁰ C, 35.0⁰ C, and 40.0⁰ C. This was a 1: 1 molar ratio between the species. Another set of reaction was carried out with a molar ratio of 1:10 between the ferrocyanide and Co complex respectively. This was carried out with a Co complex molarity of 3.0×10^{-4} M and a ferrocyanide solution molarity of 0.20 M. Absorbance readings were taken after every minute for 15 minutes. This absorbance was subtracted from the maximum absorbance. A plot of $\ln (A_{\text{max}}-A_t)$ versus time (seconds) gave a slope of $'-k_{\text{obs}}'$, the observed rate constant. This process was repeated for the various temperatures and results replicated. From the observed rate constants, we plotted the data were plotted using both Arrhenius and Eyring's equations to obtain the activation parameters; energy of activation (Ea), entropy of activation (ΔS^\ddagger), and enthalpy of activation (ΔH^\ddagger) of the two reacting species.

CHAPTER 3

RESULTS

In our research, we improved the synthesis of $K[Co(HEDTA)NO_2]$ over the published method³ and also investigated several activation parameters of the oxidation reaction between ferrocyanide and $K[Co(HEDTA)NO_2]$.

We used various analytical methods to characterize and confirm the identity and purity of $K[Co(HEDTA)NO_2]$. First, we used the UV-Vis to get the plot of the absorbance of a given concentration of the complex. From this plot, we calculated the molar extinction coefficient of the complex. This was used to characterize as well as determine the purity of the complex.

Using the Beer-Lambert law, the absorbance divided by the concentration equals a constant known as the molar extinction coefficient, ϵ , given a path length (1 cm). A less pure compound is expected to absorb less at a given wavelength, hence giving rise to a lower molar extinction coefficient. Two solutions, 3.677×10^{-3} M and 1.725×10^{-3} M of $K[Co(HEDTA)NO_2]$, produced a molar extinction coefficient of $230.4 \text{ dm}^3 \text{ mol}^{-1} \text{ cm}^{-1}$ at 495 nm. The literature value³ is 232.0. This gave us a purity of 99.3%. This was a clear indication that Beer's law was obeyed and that the precipitate was pure $K[Co(HEDTA)NO_2]$.

The next method of characterization used the IR spectrum to determine the presence, position and orientation of the nitro group in the complex. The IR showed a peak 1334.52 cm^{-1} . This confirmed two things about the complex; first, it confirmed the presence of a nitro group in the complex and secondly, it confirmed the kind of bonding the nitro group had with the Co

complex. If the NO_2 group present in the complex had the N bonded to the Co center, the literature⁴ value for the peak position was given to be 1335 cm^{-1} . On the other hand, if we had the O in NO_2 bonded to the Co center, the peak position from the literature value is the at 1428 cm^{-1} . Hence, comparing our peak of 1334.52 cm^{-1} , we realized that we had the N bonded to the Co because our value was approximately equal to the literature value for N in the nitro group. The spectrum is illustrated in Figure 2 below. This second characterization confirmed the presence of the nitro group in our complex and also confirmed the type of bonding existing between the NO_2 and the Co center.

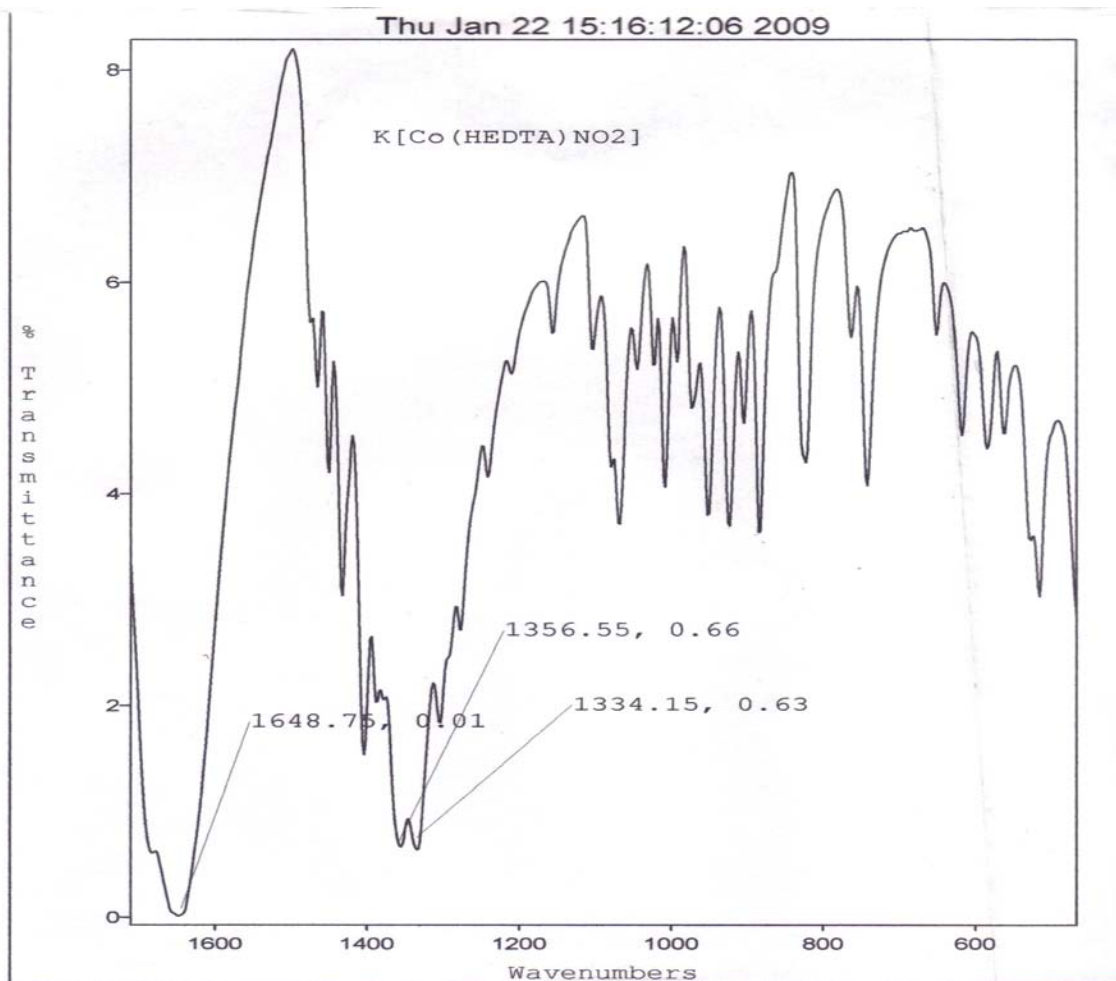


Figure 2. The Plot of the Percent Transmittance vs Wave Numbers of $\text{K}[\text{Co}(\text{HEDTA})\text{NO}_2]$.

From the UV-Vis and IR, we confirmed the purity of the complex. We also confirmed the presence of the nitro group. The position of the nitro group in our complex was further confirmed by comparing our value for UV-Vis with the literature and related research. When the nitro group is present in the axial position, the complex absorbs light at a wavelength of 495 nm with its extinction coefficient at $232 \text{ dm}^3 \text{ mol}^{-1} \text{ cm}^{-1}$. If the nitro group is in the equatorial position in the complex, the complex absorbs light at a higher wavelength² (530nm). Our peak corresponds to the nitro group in the axial position as it absorbs at 495nm, opposed to the equatorial position. This was the last step used to complete the characterization of the complex. The structure of the complex is illustrated in the UV-Vis spectrum in Figure 3 below.

The rate constants of the reaction at various temperatures were determined. This process was repeated for the various temperatures and results replicated. Ferricyanide is the product of the oxidation of ferrocyanide and as the ferricyanide evolves, it is detected by the absorption spectroscopy. A ferricyanide solution of $9.384 \times 10^{-4} \text{ M}$ of ferricyanide made from fresh grade $\text{K}_3[\text{Fe}(\text{CN})_6]$, gave a spectral peak at 420 nm with a molar extinction coefficient of $1023 \text{ dm}^3 \text{ mol}^{-1} \text{ cm}^{-1}$, which is in agreement with the literature value⁵.

The reaction was carried out at constant ionic strength by using a Na_3PO_4 buffer. In order to prevent oxidation, all solutions were properly degassed with Ar and containers sealed with a rubber septum. The concentration of buffer and inert electrolyte is very important. This is because the phosphate molecule, if present in high concentration will complex with Fe^{+3} that causes a breakdown of the ferrocyanide thereby producing erroneous results. Therefore, we maintained a buffer concentration of 0.01 M.

We then carried out a series of experiments to determine if the reaction went to completion or resulted in equilibrium. Solutions of $[\text{Co}(\text{HEDTA})\text{NO}_2]^-$ with ferrocyanide of 0.00030M, 0.00045 M, 0.00060 M and 0.0020 M were reacted with a range of 4.5 to 333 molar excess of ferrocyanide. The theoretical maximum absorbance at 423nm where $\epsilon = 1023 \text{ cm}^{-1} \text{ M}^{-1}$, assuming complete conversion to product was then compared with the actual maximum absorbance. The data are illustrated in Table 1 below while the spectrum is illustrated in Figure 3.

Table 1. Percent of Reaction Completion Between ferrocyanide and Co Complex .

The pH of solution was 6.00, ferrocyanide concentration was 0.1 except for * where the was 0.009 M.

Molarity of $\text{K}[\text{Co}(\text{HEDTA})\text{NO}_2]$	Excess molarity of $\text{K}_4[\text{Fe}(\text{CN})_6]$	Theoretical A_{max}	Actual A_{max}	Percent of completion
3.00×10^{-4}	333	0.307	0.302	98%
4.50×10^{-4}	222	0.460	0.421	91%
6.00×10^{-4}	166	0.614	0.516	84%
2.00×10^{-3}	50.0	2.05	1.141	55%
2.00×10^{-3}	4.50*	2.05	0.703	34%

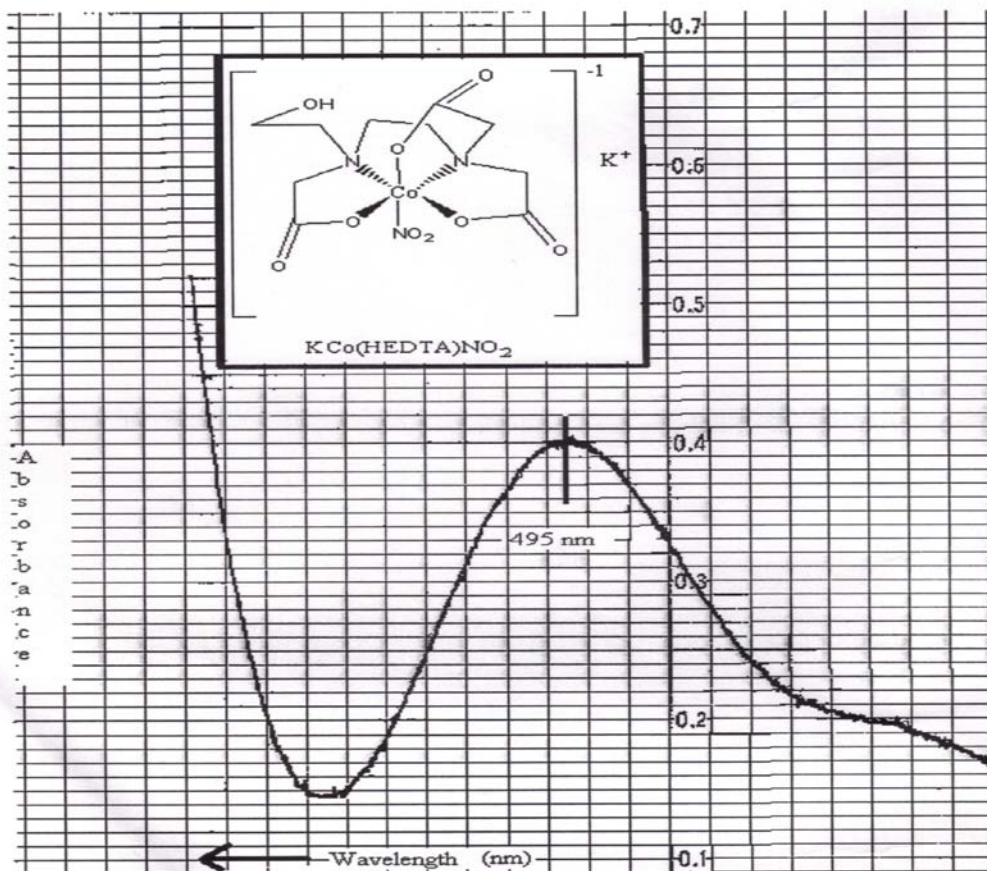


Figure 3. The Spectrum¹ of $K[Co(HEDTA)NO_2]$ at Wavelength Range of 400 nm-600 nm at pH 6.

The concentration of $K[Co(HEDTA)NO_2]$ is 0.0017 M.

The same experimental procedure was repeated at temperatures 25.0⁰ C, 27.5⁰ C, 30.0⁰ C, 35.0⁰ C, and 40.0⁰ C. The plot illustrating the change in absorbance with respect to time (seconds) was similar for all temperature. This plot is represented in Figure 4 below.

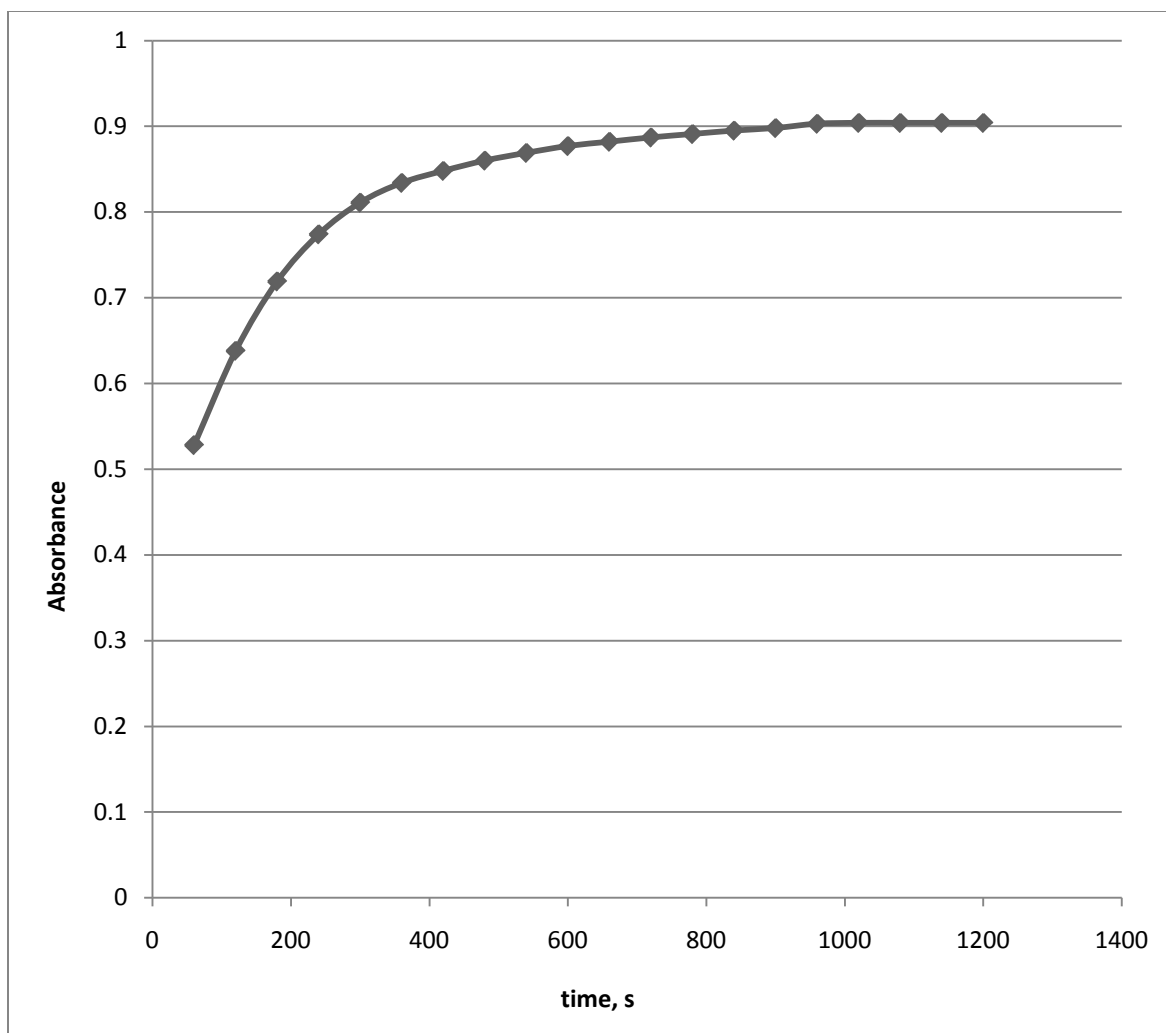


Figure 4. Plot of Absorbance (A_{420}), vs Time of the Reaction Between Ferrocyanide and $[\text{Co}(\text{HEDTA})\text{NO}_2]^-$.

From the data, the plot of $\ln(A_{\text{max}} - A_t)$ vs time gave the rate constants at the respective temperatures. The plot is illustrate in Figure 5.

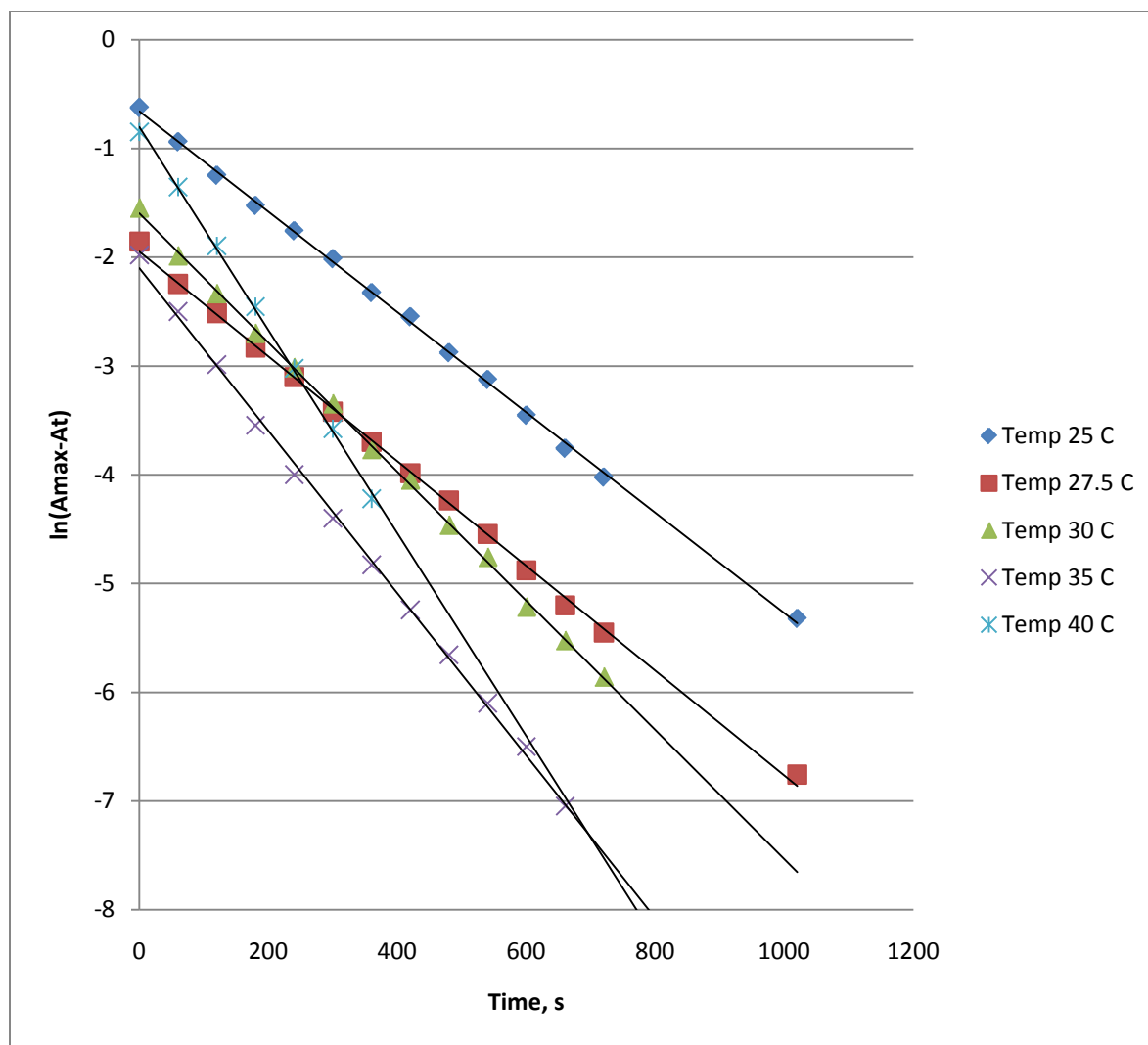


Figure 5. The Plot of $\ln(A_{\max}-A_t)$ vs Time for a 1:1 Molar Ratio.

The rate constants at the respective temperatures 25.0⁰ C, 27.5⁰ C, 30.0⁰ C, 35.0⁰ C, and 40.0⁰ C for the 1:1 molar ratio are represented in Table 2 below.

Table 2. Observed Rate Constant and Temperature for the 1:1 Molar Ratio.

Temperature, K	298.0k	300.5k	303.0k	308.0k	313.0k
Observed rate constant, s ⁻¹	0.0027	0.0029	0.0035	0.0044	0.0055

After getting the rate constant, k , we proceeded to get the activation parameters of the reacting complexes. We used the Arrhenius equation and plotted $\ln(k)$ vs $1/T$ (K^{-1}) to get the energy of activation E_a . The plot is illustrated in Figure 6.

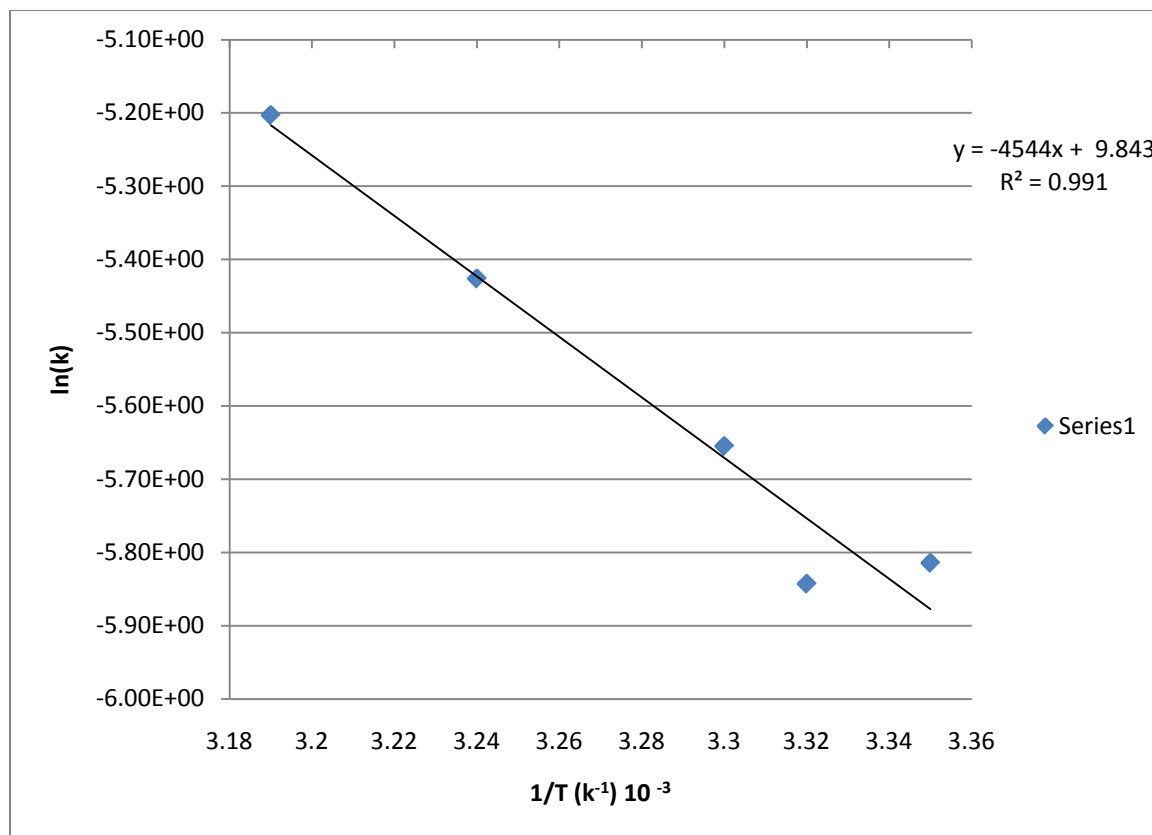


Figure 6. Plot of $\ln(k)$ vs $1/T$ (K^{-1}) for the 1:1 Molar Ratio.

From the plot, the slope = $-E_a/R$ and we calculated the energy of activation (E_a) to equal 34.8 KJ/mol. This value falls within the range of values of redox reactions of this type as represented in the literature.

We then used the Eyring's equation;

$$k = \left(\frac{k_B T}{h} \right) \exp \left(\frac{\Delta S^\ddagger}{R} \right) \exp \left(-\frac{\Delta H^\ddagger}{RT} \right)$$

This is rearranged to

$$\ln \frac{k}{T} = \frac{-\Delta H^\ddagger}{R} \cdot \frac{1}{T} + \ln \frac{k_B}{h} + \frac{\Delta S^\ddagger}{R}$$

We used our data to plot $\ln(k/T)$ vs $1/T$ in order to get the enthalpy of activation (ΔH^\ddagger), and the entropy of activation (ΔS^\ddagger), and the plot is represented in Figure 7.

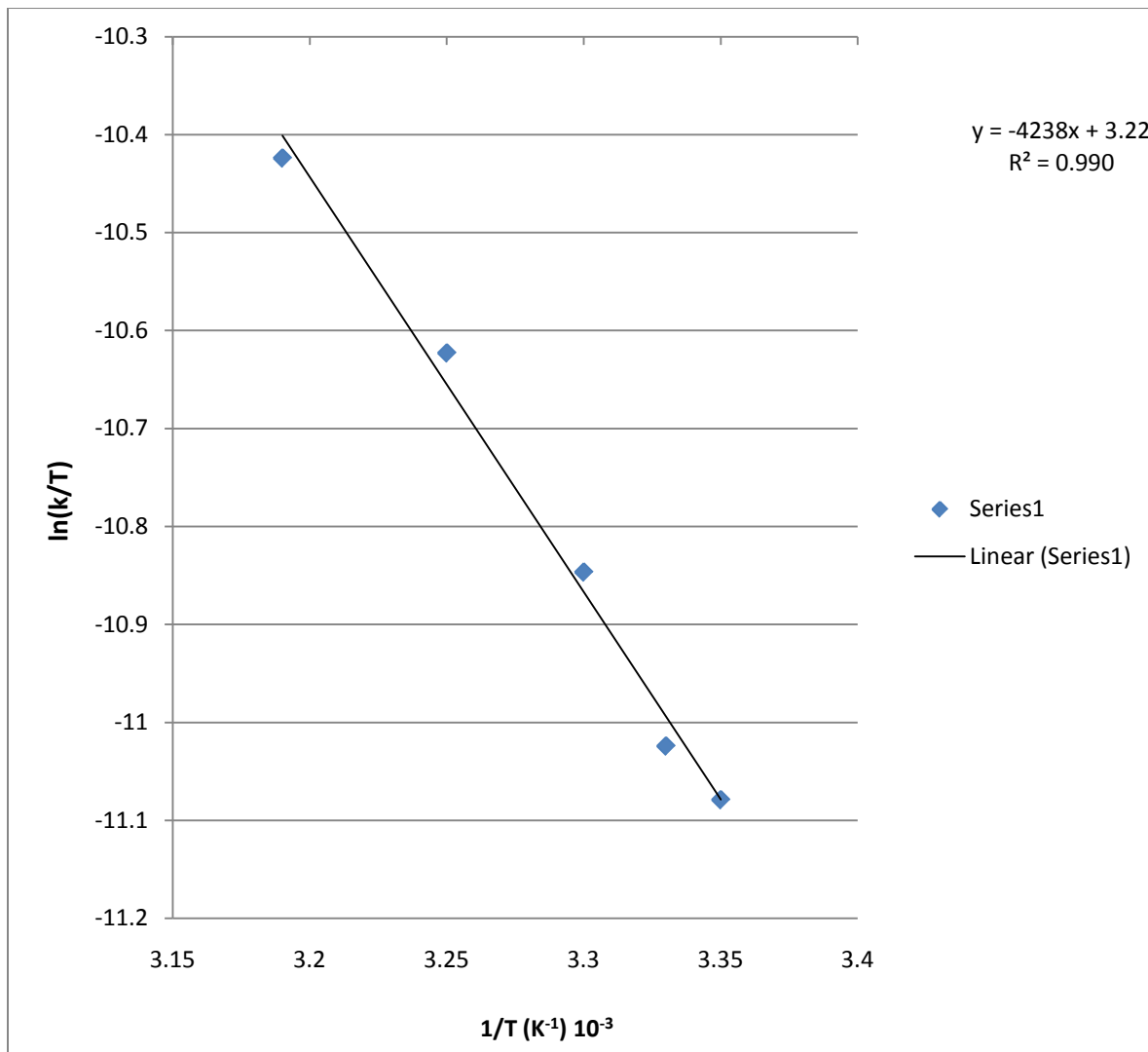


Figure 7. Plot of $\ln(k/T)$ vs $1/T$ for the 1:1 Molar Ratio.

From the Eyring equation, the slope $= -(\Delta H^\ddagger)/R$ was calculated and ΔH^\ddagger equal 34.42 kJ/mole. From the intercept, we got the entropy to equal 170.3 J/mol K.

In the second set of experiments, we used a 1:10 ratio between the $K_4[Fe(CN)_6]$ and $K[Co(HEDTA)NO_2]$ to obtain pseudo first order conditions. From the data, the plot of $\ln(A_{max}-A_t)$ vs time gave the rate constants at the respective temperatures. The plot is illustrate in Figure 8.

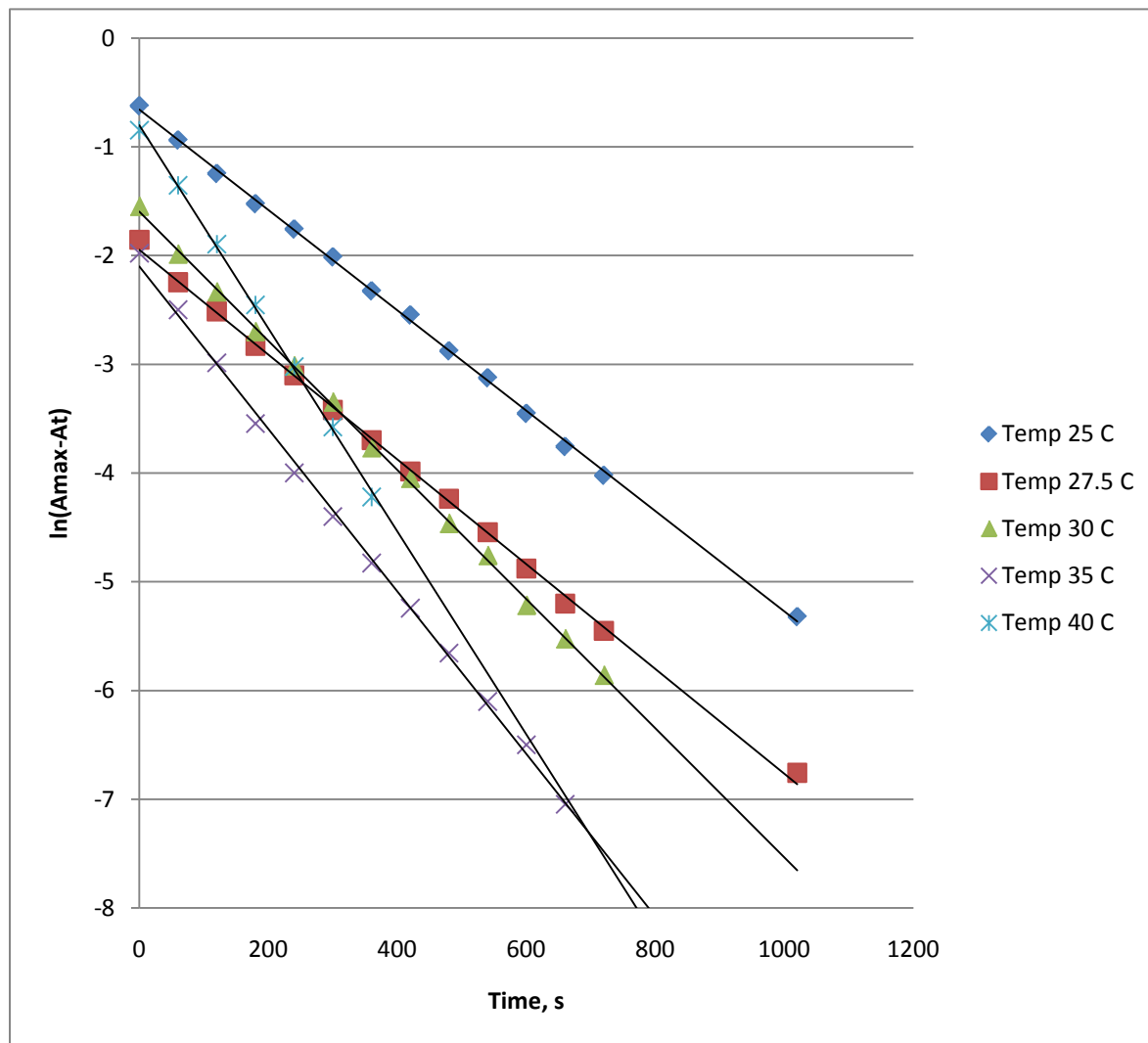


Figure 8. The Plot of $\ln(A_{max}-A)$ vs Time for 1:10 Molar Ratio.

The rate constants at the respective temperatures $25.0^{\circ}C$, $27.5^{\circ}C$, $30.0^{\circ}C$, $35.0^{\circ}C$, and $40.0^{\circ}C$ for the 1:10 molar ratio are represented in Table 3 below.

Table 3. The Observed Rate Constants at Different Temperatures for 1:10 Ratio

Temperature, K	298.0k	300.5k	303.0k	308.0k	313.0k
Observed rate constant, s^{-1}	0.0046	0.004	0.0059	0.0075	0.0093

After getting the rate constant, k , we proceeded to get the activation parameters of the reacting complexes. We used the Arrhenius equation and plotted $\ln(k)$ vs $1/T(K^{-1})$ to get the energy of activation, E_a . The plot is illustrated in Figure 9.

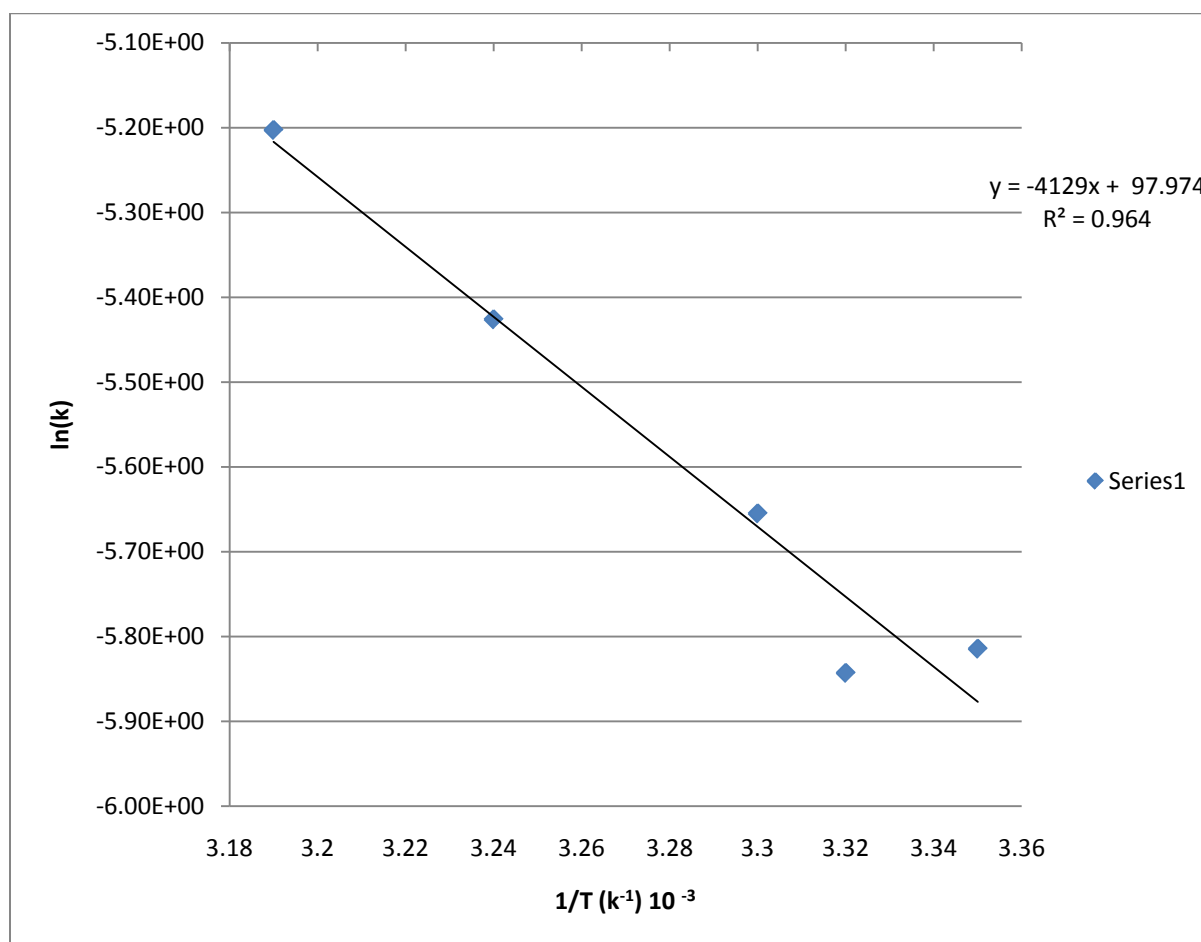


Figure 9. Plot of $\ln(k)$ vs $1/T (K^{-1})$ for the 1:10 Molar Ratio.

we calculated the energy of activation (E_a) to equal 34.3 KJ/mol.

We then used the Eyring's equation and plotted $\ln(k/T)$ vs $1/T$ in order to get the enthalpy of activation (ΔH^\ddagger), and the entropy of activation (ΔS^\ddagger) as illustrated in Figure 10.

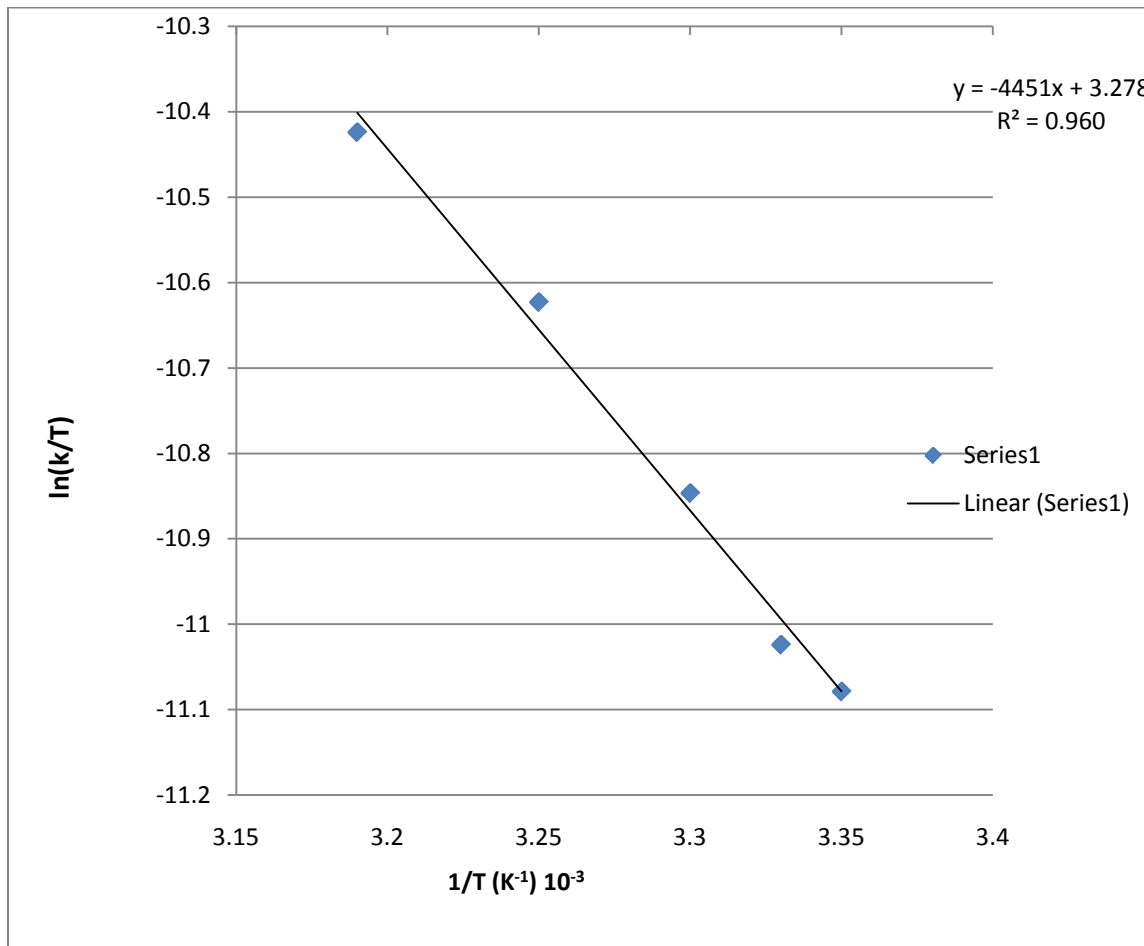


Figure 10. Plot of $\ln(k/T)$ vs $1/T (\text{K}^{-1})$ for the 1:10 Molar Ratio.

From the Eyring equation, we calculated ΔH^\ddagger to equal 37.00 kJ/mole and from the intercept we calculated the entropy to equals 171.6 J/mol K.

CHAPTER 4

DISCUSSION

From the absorbance plot of $K[Co(HEDTA)NO_2]$, we calculated the molar extinction coefficient using the Beer's law. Our value ($230 \text{ dm}^3 \text{ mol}^{-1} \text{ cm}^{-1}$) was calculated to be 99.3% of the literature value of $232 \text{ dm}^3 \text{ mol}^{-1} \text{ cm}^{-1}$ at wavelength of 495 nm. This was important evidence that our product was the $K[Co(HEDTA)NO_2]$. Furthermore, by using the IR, we determined that N in the nitro group was bonded to the Co center. This was done by obtaining a peak position of 1334.52 cm^{-1} , which when compared with literature value⁴ (1335 cm^{-1}) confirmed the fact that N in the nitro group was indeed the bonded element to the Co center. This further supported the fact that our product was pure $K[Co(HEDTA)NO_2]$. These procedures and their results clearly indicated that our product was properly synthesized and also in its pure form.

From our experiments, the unchanged absorbance of the ferrocyanide in a degassed buffer solution of pH 6 indicated that the complex was stable without the presence of air. Likewise, $K[Co(HEDTA)NO_2]$ stability is also indicated as its spectrum remains unchanged over the time in the course of the runs.

Table 1 gives the observed percent reaction between the complexes at different molar ratios. As indicated, the percent completion is low when the molar ratio between the species is small and high when the molar ratio is large. In the case where the molar ratios between the two complexes is less than 10, the maximum absorbance does not equal the molarity of the

limiting reagent $K[Co(HEDTA)NO_2]$ multiplied by the molar extinction coefficient of ferricyanide ($1023 \text{ dm}^3 \text{ mol}^{-1} \text{ cm}^{-1}$). This means that the reaction at low molar ratios between the complexes exists at equilibrium which is further indicated by the low percent completion of the reaction. Nevertheless, when the molar ratio is large (1:10), with ferrocyanide in excess, the maximum absorbance is approximately equal to the molarity of the limiting reagent $K[Co(HEDTA)NO_2]$ multiplied by the molar extinction coefficient for ferricyanide. This is showed by the high percent completions at these molar ratios. This means that at a high molar ratio, we have a pseudo first order reaction between the limiting reagent $K[Co(HEDTA)NO_2]$ and the ferrocyanide in excess. The reaction therefore goes very close to completion and we have an overall high percent completion.

Former research ¹ indicated a first order behavior for each reactant. From Tables 2 and 3, we clearly show that the rate constants increase as the temperature increases. All duplicated data were supportive of this idea. This further complemented the early research in the fact that we now know with high certainty, and with backing from our data and plots that, the first order reactant rate constants increases with temperature. These plots further allow us to get succinct information of the activation parameters of the reacting species.

The time needed to remove the cuvettes from the temperature bath and eject and inject solutions was varied from 3 to 4 seconds, that came with many trials and practice. The time for mixing and initiating the UV-Vis scans introduced determinate errors in our result that was unavoidable.

Figures 5 and 8 show the logarithmic evolution of ferrocyanide with time as we plotted $\ln(A_{max}-A)$ vs time, giving us the observed rate constants in the two cases at the respective temperatures. The observed rate constants were then used in accordance with the Arrhenius equation and also the Eyring equations to obtain the E_a , ΔS^\ddagger , and ΔH^\ddagger for the two reacting complexes. The value of the enthalpy of activation 34.42 KJ/mol for the 1:1 ratio which is lower than that of the 1:10 molar ratio is indicative of the fact that at equilibrium, the rate of conversion of reactants to products is comparable to the rate of conversion of products to reactants. Hence, at that specified temperature as indicated by the Arrhenius equation, as a result of the kinetic equilibrium between reactants and products, the enthalpy of activation for the product formation is low. In the case of the 1:10 ratio the enthalpy of activation is high (37.00 KJ/mol) because one reacting species, $K[Co(HEDTA)NO_2]$, is limited and so the excess ferrocyanide reacts with most of the $K[Co(HEDTA)NO_2]$ to form the product. As a result, the reaction goes to completion thereby having a higher enthalpy of activation. This idea is in conformity with other related research ²of compounds of this nature and the value of E_a and positive values ΔS^\ddagger and ΔH^\ddagger , are in the range expected on the basis of literature values ². Table 4 illustrated below contains activation parameters for the 1:1 and 1:10 molar ratios.

Table 4. Activation Parameters for 1:1 and 1:10 Molar Ratios.

Activation parameters for 1:1 ratio	Activation parameters for 1:10 ratio
• $E_a = 34.8\text{KJ/mol}$	• $E_a = 34.3\text{KJ/mol}$
• $\Delta H^\ddagger = 35.24\text{kJ/mole}$	• $\Delta H^\ddagger = 37.00\text{kJ/mole}$
• $\Delta S^\ddagger = 170.3\text{J/mol K.}$	• $\Delta S^\ddagger = 171.6\text{J/mol K.}$

These values correspond with the line of thought that the solvation spheres of both reacting species undergo little modification to the extent that the process of electronic transfer occurs with the minimum change in their coordination spheres. This is in accordance with the Frank-Condon principle that states for any vertical electronic transition, the time it takes an electron to be transferred between the two species is 10^{-15} seconds which is faster than any molecular motion, hence the molecule remains unchanged during the transfer. The positive value of the ΔS^\ddagger is a clear indication of an outer-sphere mechanism. This is because in the transition state for an outer-sphere the two complexes are not linked together. They are free to move randomly giving rise to positive ΔS^\ddagger . For an inner-sphere mechanism, the complexes are linked together by a bridging ligand, hence do not move freely. This gives rise to negative ΔS^\ddagger for inner-sphere mechanisms. This confirms the values of similar research² and further confirms our conclusion that the outer-sphere mechanism is the path way of the electron transfer.

Pertaining to our reaction and activation parameters, the rate of electronic transfer is greater than the reorganization energy of the two reacting species. Therefore, the electron transfer occurs with minimum change from the coordination sphere of the reactants. This in turn means that the electronic transfer occurs without bond breaking and formation, which favors outer-sphere mechanism as the mechanistic pathway over inner-sphere mechanism. This is supported by Marcus theory. Because both species are octahedral low spin ' $3d^6$ ' species, they both undergo very little internal reorganization. This means little rearrangement energy between the species in the transition state, which in turn increases electronic transition.

In Inner-sphere mechanism there is a formation of a bridge between the reacting species which facilitates electronic transfer. This is made possible by a bridging ligand, hence for the product ferricyanide to be formed, bonds would have to be formed and broken at the activation complex in the transition state. Hence, one of the ligands in the $K[Co(HEDTA)NO_2]$ would have to be dissociated. If this were the case then the spectrum of the $K[Co(HEDTA)NO_2]$ would have been different because it would result to a different structural molecule. But because the spectrum did not change over the period of the redox reaction, no ligand dissociation occurred. This further indicates the preference of an outer-sphere over the inner-sphere mechanism.

In similar studies of compounds of this nature^{2,3}, the rate of inner sphere mechanism is 200 times faster than our results. The rate of outer-sphere mechanism between a positive and a negatively charge species is 30 times faster than our results. Because we are dealing with two negatively charge species, the rate of electronic transfer is expected to be the slowest due to repulsion. Related research² have activation parameters; ΔH^\ddagger ranging from 87 – 102 KJ/mol, ΔS^\ddagger ranging from 27 KJ/mol – 95 KJ/mol with values of rate constants ranging from 11 s^{-1} to 3500 s^{-1} . This research was done at a low pH of 3.8 and was carried out in order to determine the correlation between the size of alkyl functions, R, and rate of reaction between the $[Co(RNH_2)_5(H_2O)]^{3+}$ and ferrocyanide. Similar research¹⁰ studied the reaction between different aminoplycarboxylates; TRDTA, CyDTA, EDTA, PDTA, and HEDTA linked to Co centers and monitored their reactions with ferrocyanide. The outer-sphere mechanism was proposed and the rate constants varied from $1.0 \times 10^{-4} \text{ s}^{-1}$ to $5.4 \times 10^{-3} \text{ s}^{-1}$. This research included the ligand we

used(HEDTA) and our values of rate constants was in the same range as that of the research which further supports our conclusion of an outer-sphere mechanism.

In conclusion, our synthesis of the kinetically-inert complex $K[Co(HEDTA)NO_2]$ has been improved to give us a purer product with higher yield (89.5%). Various activation parameters E_a , ΔS^\ddagger , and ΔH^\ddagger have been determined and data replicated for the reaction between $K[Co(HEDTA)NO_2]$ and the ferrocyanide. From the activation parameters and from other research¹, we have been able to conclude that the electronic transfer between $K[Co(HEDTA)NO_2]$ and ferrocyanide occurs by an outer-sphere mechanism.

Future areas of study include exploration for the reduced form of $[Co(HEDTA)NO_2]^-$. The structural change associated with the reduction is not yet known and also the specific location of reduction on the molecule is yet to be determined. As a result of the high lability of the $[Co(HEDTA)NO_2]^{2-}$, it is very hard to isolate it in solution. Advance techniques and instrumentation (may be trapping) may allow us to isolate and study it. This might be beneficial to the world of science and will take us closer to a clearer understanding of species and reactions of this nature.

BIBLIOGRAPHY

1. David L. Burrows *The Kinetics and Mechanism of $[\text{Co}(\text{HEDTA})\text{NO}_2]^{-1}$ and $\text{Fe}(\text{CN})_6]^{-4}$* ; **2000**, 1-36. Thesis ETSU.
2. Martinez, M., Pitarque, M., and Eldik. R. *J. Chem. Soc. Dalton Trans.* **1994**, 3159-3163.
3. Morris, M. L., and Busch, D. H. *J. Amer. Chem. Soc.* **1956**, 78, 5178-5181.
4. Kazuo Nakamoto, *Infrared Spectra of Inorganic and Coordination Compounds*, John Wiley & Sons, Inc. 4th edition **1963**, 150.
5. Martinez, M., Pitarque, M., and Eldik. R. *J. Chem. Soc. Dalton Trans.* **1994**, 3159-3163.
6. I. Krack and Eldik R. Van, *Inorg. Chem.*, **1990**, 29, 549.
7. A. L. Seligson and W. C. Trogler, *J. Am. Chem. Soc.*, **1991**, 113, 2520.
8. D. Gaswick and A. Haim, *J. Am. Chem. Soc.*, **1971**, 93, 7347.
9. D. D. Perrin, *Aust. J. Chem.*, **1963**, 16, 372.
10. Hiroshi. O, T. Masatake, Nobuyuki. *Japan. Chem. Soc.*, **1974**, 47(6), 1426-1429.

APPENDICES

Appendix A: The Data for Absorbance vs Temperatures for 1:1 Molar Ratio

Time, seconds(25.0 ⁰ C)	Absorbance(25.0 ⁰ C)	Time, seconds (27.50 ⁰ C)	Absorbance(27.5 ⁰ C)
0.00	0.324	0.00	0.327
60.0	0.406	60.0	0.395
120.0	0.483	120.0	0.477
180.0	0.537	180.0	0.539
240.0	0.577	240.0	0.589
300.0	0.606	300.0	0.633
360.0	0.630	360.0	0.666
420.0	0.648	420.0	0.695
480.0	0.664	480.0	0.719
540.0	0.678	540.0	0.744
600.0	0.689	600.0	0.779
720.0	0.709	720.0	0.793
900.0	0.734	900.0	0.829
1020	0.748	1020	0.848

Time,seconds (30.0 ⁰ C)	Absorbance (30.0 ⁰ C)	Time,seconds (35.0 ⁰ C)	Absorbance (35.0 ⁰ C)	Time,seconds (40.0 ⁰ C)	Absorbance (40.0 ⁰ C)
0.00	0.394	0.00	0.496	0.00	0.752
60.0	0.480	60.0	0.615	60.0	0.802
120.0	0.576	120.0	0.705	120.0	0.904
180.0	0.641	180.0	0.756	180.0	0.962
240.0	0.687	240.0	0.785	240.0	0.995
300.0	0.721	300.0	0.806	300.0	1.020
360.0	0.748	360.0	0.821	360.0	1.039
420.0	0.770	420.0	0.833	420.0	1.055
480.0	0.789	480.0	0.844	480.0	1.070
540.0	0.805	540.0	0.853	540.0	1.083
600.0	0.820	600.0	0.861	600.0	1.093
720.0	0.844	720.0	0.874	720.0	1.112
900.0	0.875	900.0	0.887	900.0	1.138
1020	0.891	1020	0.894	1020	1.490

Appendix B: The Data for Absorbance vs Temperatures for 1:10 Molar Ratio:

Time, seconds(25.0 ⁰ C)	Absorbance(25.0 ⁰ C)	Time, seconds (27.50 ⁰ C)	Absorbance(27.5 ⁰ C)
0.00	0.371	0.00	0.475
60.0	0.516	60.0	0.557
120.0	0.624	120.0	0.611
180.0	0.709	180.0	0.633
240.0	0.763	240.0	0.652
300.0	0.801	300.0	0.644
360.0	0.826	360.0	0.654
420.0	0.834	420.0	0.652
480.0	0.859	480.0	0.660
540.0	0.864	540.0	0.671
600.0	0.872	600.0	0.674
660.0	0.864	660.0	0.676
720.0	0.872	720.0	0.678
1020	0.900	1020	0.690

Time,seconds (30.0 ⁰ C)	Absorbance (30.0 ⁰ C)	Time,seconds (35.0 ⁰ C)	Absorbance (35.0 ⁰ C)	Time,seconds (40.0 ⁰ C)	Absorbance (40.0 ⁰ C)
0.00	0.583	0.00	0.734	0.00	1.3343
60.0	0.716	60.0	0.809	60.0	1.5049
120.0	0.788	120.0	0.836	120.0	1.6120
180.0	0.826	180.0	0.850	180.0	1.6771
240.0	0.849	240.0	0.859	240.0	1.7143
300.0	0.869	300.0	0.863	300.0	1.7350
360.0	0.863	360.0	0.865	360.0	1.7483
420.0	0.870	420.0	0.868		
480.0	0.876	480.0	0.869		
540.0	0.877	540.0	0.870		
600.0	0.879	600.0	0.871		
720.0	0.881	660	0.872		
840.0	0.883				

All data were replicated and values of activation parameters were similar in all cases with respect to the blank.

VITA

SAMMY ENI ENI

Personal Data: Date of Birth; August 20th, 1984.
 Place of Birth; Kumba, Cameroon.
 Marital Status; Single.

Education: Primary School; St. John Primary school.
 Secondary and High School; Bishop Rogan Minor Seminary.
 Universities; University of Buea, Cameroon BS. September 2006.
 East Tennessee State University. MS. December 2009.

Professional Experience: National Oil Refinery, Limbe, Cameroon, 2006-2008
 Graduate Assistant, East Tennessee State University,
 College of Arts and Sciences, 2008-2009.